

# The topology of higher-order complexes associated with brain-function hubs in human connectomes

Miroslav Andjelković<sup>a,b</sup>, Bosiljka Tadić<sup>a,d</sup>, Roderick Melnik<sup>c,e</sup>

<sup>a</sup>Department of Theoretical Physics, Jožef Stefan Institute, Ljubljana, Slovenia;

<sup>b</sup>Institute for Nuclear Sciences Vinča, University of Belgrade 11000 Belgrade, Serbia;

<sup>c</sup>MS2Discovery Interdisciplinary Research Institute, M2NeT Laboratory  
and Department of Mathematics, Wilfrid Laurier University, Waterloo, ON, Canada;

<sup>d</sup>Complexity Science Hub, Josefstädter Strasse 39, Vienna, Austria;

<sup>e</sup>BCAM - Basque Center for Applied Mathematics, Alameda de Mazarredo 14, E-48009 Bilbao, Spain

bosiljka.tadic@ijs.si, <http://www-f1.ijs.si/~tadic/>

## Contents

<b>1</b>	<b>Introduction</b>	<b>2</b>
<b>2</b>	<b>Methods</b>	<b>3</b>
2.0.1	Data description . . . . .	3
2.0.2	Topology analysis and definition of quantities . . . . .	4
2.0.3	Network structure & hyperbolicity . . . . .	5
<b>3</b>	<b>Results</b>	<b>6</b>
3.1	Whole-brain connectomes: Identification of hubs from topological dimension . . . . .	6
3.2	Core networks associated with global hubs in the female and male connectomes . . . . .	7
3.3	Topology of core networks depending on the weights of edges . . . . .	8
<b>4</b>	<b>Discussion and Conclusions</b>	<b>11</b>

## Abstract

Higher-order connectivity in complex systems described by simplexes of different orders provides a geometry for simplex-based dynamical variables and interactions. Simplicial complexes that constitute a functional geometry of the human connectome can be crucial for the brain complex dynamics. In this context, the best-connected brain areas, designated as hub nodes, play a central role in supporting integrated brain function. Here, we study the structure of simplicial complexes attached to eight global hubs in the female and male connectomes and identify the core networks among the affected brain regions. These eight hubs (Putamen, Caudate, Hippocampus and Thalamus-Proper in the left and right cerebral hemisphere) are the highest-ranking according to their topological dimension, defined as the number of simplexes of all orders in which the node participates. Furthermore, we analyse the weight-dependent heterogeneity of simplexes. We demonstrate changes in the structure of identified core networks and topological entropy when the threshold weight is gradually increased. These results highlight the role of higher-order interactions in human brain networks and provide additional evidence for (dis)similarity between the female and male connectomes.

*Keywords:* Brain-function hubs, Human connectomes, Higher-order networks

## 1 Introduction

Recent advances in the science of complex systems aim for a better understanding of the higher-order connectivity as a possible basis for their emerging properties and complex functions. Beyond the framework of pairwise interactions, these connections described by simplexes of different sizes provide the geometry for higher-order interactions and simplex-related dynamical variables. One line of research consists of modelling and analysis of the structure of simplicial complexes in many complex systems, ranging from the human connectome [1] to quantum physics [2] and materials science [3, 4]. Meanwhile, considerable efforts aim at understanding the impact of geometry on the dynamics. In this context, the research has been done on modelling of the simplex-based synchronisation processes [5, 6], on studying the related spectral properties of the underlying networks [7, 8], as well as on the interpretation of the dynamics of the brain [9, 10, 11] and other complex dynamical systems [12].

Recently, mapping the brain imaging data [13] to networks involved different types of signals across spatial and temporal scales; consequently, a variety of structural and functional networks have been obtained [14, 15, 16, 17]. This network mapping enabled getting a new insight into the functional organisation of the brain [18, 19], in particular, based on the standard and deep graph theoretic methods [20, 21, 22] and the algebraic topology of graphs [1, 23]. The type of network that we consider in this work is the whole-brain network *human connectome*; it is mapped from the *fMRI* data available from the human connectome project [24], see Methods. The network nodes are identified as the grey-matter anatomical brain regions, while the edges consist of the white-matter fibres between them. Beyond the pairwise connections, the human connectome exhibits a rich structure of simplicial complexes and short cycles between

them, as it was shown in [1]. Furthermore, on a mesoscopic scale, a typical structure with anatomical modules is observed. It has been recognised [25, 26] that every module has an autonomous function, which contributes to performing complex tasks of the brain. Meanwhile, the integration of this distributed activity and transferring of information between different modules is performed by very central nodes (hubs) as many studies suggest, see a recent review [11] and references therein. Formally, hubs are identified as a group of four or five nodes in each brain hemisphere that appear as top-ranking according to the number of connections or another graph-centrality measure. Almost all formal criteria give the same set of nodes, which are anatomically located deep inside the brain, through which many neuronal pathways go. Recently, there has been an increased interest in the research of the hubs of the human connectome. The aim is to decipher their topological configuration and how they fulfil their complex dynamic functions. For example, it has been recognised that the brain hubs are mutually connected such that they make a so-called “rich club” structure [27]. Moreover, their topological configuration develops over time from the prenatal to childhood and adult brain [28, 29]. The hubs also can play a crucial role in the appearance of diseases when their typical configuration becomes destroyed [30].

Assuming that the higher-order connectivity may provide a clue of how the hubs perform their function, here we examine the organisation of simplicial complexes around eight leading hubs in the human connectome. Based on our work [1], we use the consensus connectomes that we have generated at the Budapest connectome server [31, 32]. These are connectomes that are common for one hundred female subjects (F-connectome) and similarly for one hundred male subjects (M-connectome), see Methods. Accordingly, we determine the hubs as eight top-ranking nodes in the whole connectome, performing the ranking according to the number of simplexes of all orders in which the node participates. These are the Putamen, Caudate, Hippocampus and Thalamus-Proper in the left and similarly in the right brain hemisphere; they also appear as hubs according to several other graph-theory measures. We then construct *core networks* consisting of these hubs and all simplexes attached to them in both female and male connectomes. We determine the simplicial complexes and the related topological entropy in these core structures. To highlight the weight-related heterogeneity of connections, the structure of these core networks is gradually altered by increasing the threshold weight above which the connections are considered as significant. We show that the connectivity up to the 6th order remains in both connectomes even at a high threshold. Meanwhile, the identity of edges and their weights appear to be different in the F- and M-connectomes.

## 2 Methods

### 2.0.1 Data description

We use the data for two *consensus connectomes* that we have generated in [1] at the Budapest connectome server 3.0 [31, 32] based on the brain imaging data from Human Connectome Project [24]. Specifically, these are the weighted whole-brain networks that are common for 100 female subjects, *F-connectome*, and similarly, *M-connectome*,

which is common for 100 male subjects. Each connectome consists of  $N = 1015$  nodes annotated as the anatomical brain regions, and weighted edges, whose weight is given by the number of fibres between the considered pair of brain regions normalised by the average fibre length. Here, we consider the largest number  $10^6$  fibres tracked and set the minimum weight to four. The corresponding core networks *Fc-network* and *Mc-network* are defined as subgraphs of the F- and M-connectomes, respectively, containing the leading hubs and their first neighbour nodes as well as all edges between these nodes. Meanwhile, the hubs are determined according to the topological dimension criteria, as described below and in Results.

## 2.0.2 Topology analysis and definition of quantities

We apply the Bron-Kerbosch algorithm [33] to analyse the structure of simplicial complexes, i.e., clique complexes, in the core Fc- and Mc- connectomes. In this context, a *simplex* of order  $q$  is a full graph (clique) of  $q + 1$  vertices  $\sigma_q = \langle i_0, i_1, i_2, \dots, i_q \rangle$ . Then a simplex  $\sigma_r$  of the order  $r < q$  which consists of  $r$  vertices of the simplex  $\sigma_q$  is a *face* of the simplex  $\sigma_q$ . Thus, the simplex  $\sigma_q$  contains faces of all orders from  $r = 0$  (nodes),  $r = 1$  (edges),  $r = 2$  (triangles),  $r = 3$  (tetrahedrons), and so on, up to the order  $r = q - 1$ . A set of simplexes connected via shared faces of different orders makes a *simplicial complex*. The order of a simplicial complex is given by the order of the largest clique in this complex, and  $q_{max}$  is the largest order of all simplicial complexes. Having the adjacency matrix of the graph, with the algorithm, we build the incidence matrix  $\Lambda$ , which contain IDs of all simplexes and IDs of nodes that make each simplex. With this information at hand, we compute three structure vectors [34, 35] to characterise the architecture of simplicial complexes:

- The *first structure vector (FSV)*:  $\mathbf{Q} = \{Q_0, Q_1, \dots, Q_{q_{max}-1}, Q_{q_{max}}\}$ , where  $Q_q$  is the number of  $q$ -connected components;
- The *second structure vector (SSV)*:  $\mathbf{N}_s = \{n_0, n_1, \dots, n_{q_{max}-1}, n_{q_{max}}\}$ , where  $n_q$  is the number of simplexes from the level  $q$  upwards;
- The *third structure vector (TSV)*: the component  $\hat{Q}_q \equiv 1 - Q_q/n_q$  quantifies the degree of connectedness among simplexes *at* the topology level  $q$ .

Furthermore, we determine the topological dimension of nodes and topological entropy introduced in [36]. The topological dimension  $dimQ_i$  of a node  $i$  is defined as the number of simplexes of all orders in which the corresponding vertex participates,

$$dimQ_i \equiv \sum_{q=0}^{q_{max}} Q_q^i, \quad (1)$$

where  $Q_q^i$  is determined directly from the  $\Lambda$  matrix by tracking the orders of all simplexes in which the node  $i$  has a nonzero entry. Then, with this information, the entropy of a topological level  $q$  defined as

$$S_Q(q) = -\frac{\sum_i P_q^i \log P_q^i}{\log M_q} \quad (2)$$

is computed. Here,  $p_q^i = \frac{Q_q^i}{\sum_i Q_q^i}$  is the node's occupation probability of the  $q$ -level, and the sum runs over all nodes. The normalisation factor  $M_q = \sum_i (1 - \delta_{Q_q^i, 0})$  is the number of vertices having a nonzero entry at the level  $q$  in the entire graph. Thus the topological entropy (2) measures the degree of cooperation among vertices resulting in a minimum at a given topology level. Meanwhile, towards the limits  $q \rightarrow 0$  and  $q \rightarrow q_{max}$ , the occurrence of independent cliques results in a higher entropy at that level.

In addition, we compute the vector  $\mathbf{f} = \{f_0, f_1, \dots, f_{q_{max}}\}$ , which is defined [36] such that  $f_q$  represents the *number of simplices and faces at the level  $q$* . Given that a free simplex of the size  $n > q$  has the corresponding combinatorial number of faces of the order  $q$ , the component  $f_q$  thus contains information about the actual number of shared faces between simplexes *at the level  $q$* .

### 2.0.3 Network structure & hyperbolicity

The underlying topological graph represents the 1-skeleton of the simplicial complex. Using the graph-theory methods [37], we determine the degree–degree correlations that are relevant to the observed "rich club behaviour" of the hubs in the global connectome [1, 27, 28, 29]. Precisely, for each node in the considered network, the average number of edges of its nearest neighbour nodes is plotted against the node's degree. The following scaling form is expected

$$\langle k \rangle_{i:nn} \sim k_i^\mu . \quad (3)$$

Here, the positive values of the exponent  $\mu > 0$  indicate the *assortative* correlations, while  $\mu < 0$  corresponds to a *disassortative* mixing, and  $\mu = 0$  suggests the absence of nodes correlations. We analyse the Fc- and Mc-graphs by considering the edges that remain after applying different weight thresholds. The weight distribution  $P(w)$  is determined for the entire core-networks, see Results.

Furthermore, using the 4-point Gromov criterion for the hyperbolic graphs [38], we determine the hyperbolicity parameter  $\delta_{max}$  of these graphs. Precisely, for each 4-tuple of nodes  $(A, B, C, D)$  in a  $\delta$ -hyperbolic graph  $G$ , the ordered relation between the sums of shortest-path distances  $\mathcal{S} \equiv d(A, B) + d(C, D) \leq \mathcal{M} \equiv d(A, C) + d(B, D) \leq \mathcal{L} \equiv d(A, D) + d(B, C)$  implies that

$$\delta(A, B, C, D) \equiv \frac{\mathcal{L} - \mathcal{M}}{2} \leq \delta(G) . \quad (4)$$

It follows from the triangle inequality that the upper bound of  $(\mathcal{L} - \mathcal{M})/2$  is given by the minimal distance  $d_{min} \equiv \min\{d(A, B), d(C, D)\}$  in the smallest sum  $\mathcal{S}$ . Thus, by sampling a large number ( $10^9$ ) 4-tuples of nodes in each graph, and plotting  $\delta(A, B, C, D)$  against the corresponding minimal distance  $d_{min}$ , we obtain  $\delta(G)$  as the upper bound of  $\delta_{max} = \max_G\{\delta(A, B, C, D)\}$ .

### 3 Results

#### 3.1 Whole-brain connectomes: Identification of hubs from topological dimension

We consider two whole-brain networks, precisely, the F-connectome, which is common for 100 female subjects, and M-connectome, consisting of the edges that are common to 100 male subjects; see Methods and [1] for more details. For illustration, the F-connectome is shown in the left panel of Figure 1. Each connectome consists of 1015 nodes as anatomical brain regions. These nodes are interconnected by a particular pattern of edges and organised in six mesoscopic communities. For this work, we determine the *global hubs* in the F- and M-connectomes. These are eight top-ranking nodes according to the number of simplexes attached to a node. Based on our work in [1], we use the corresponding  $\Lambda$ -matrix for the F- and M-connectomes and identify simplexes of all orders in which a particular node  $i = 1, 2, \dots, 1015$  participates. The node's topological dimension  $\dim Q_i$ , defined by (1) is then computed. For both connectomes, the node's ranking distribution by the decreasing topological dimension is shown in the middle right panel of figure 1. As the figure demonstrates, the eight top-ranking nodes (marked along the curve for the F-connectome) make a separate group compared to the rest of the curve. These nodes also appear (see the list below) among the first eight ranked topological hubs in the M-connectome:

rank_F	name	rank_M
1	Left Putamen	1
2	Right Putamen	3
3	Left Caudate	2
4	Right Caudate	4
5	Left Thalamus-Propper	5
6	Left Hippocampus	7
7	Right Hippocampus	8
8	Right Thalamus-Propper	6

For comparisons with other approaches, we also show that these nodes (with altered order) also appear as eight hubs ranked according to the node's strength  $S_i$ , defined as the sum of weights of all edges of the node  $i$ . In this case, the ranking curves of the F- and M-connectomes virtually overlap, see the top right panel in figure 1. The lower right panel shows the 3-dimensional plot of the node's topological dimension over different topology levels  $q$ . In this plot, the high peaks corresponding to our hubs indicate what orders of simplexes mostly contribute to distinguishing the hubs from the rest of the surrounding nodes. Note that these eight nodes also appear as the leading hubs in several other sorting methods, for example, according to the node's degree and centrality measures [29, 27]. For comparisons with other methods, we also show the names of nodes that rank from 9-20 according to the topological dimension in the case of the F-connectome:

rh.precentral\_7, Right-Pallidum, rh.caudalmiddlefrontal\_11,  
lh.caudalmiddlefrontal\_13, Brain-Stem, Left-Pallidum,

lh.precentral\_21, lh.precentral\_6, lh.superiorparietal\_25,  
rh.precentral\_19, rh.precentral\_15, rh.superiorparietal\_13

The nodes listed in the first two rows, except from the Brain Stem, also appear in this ranking range in the M-connectome.

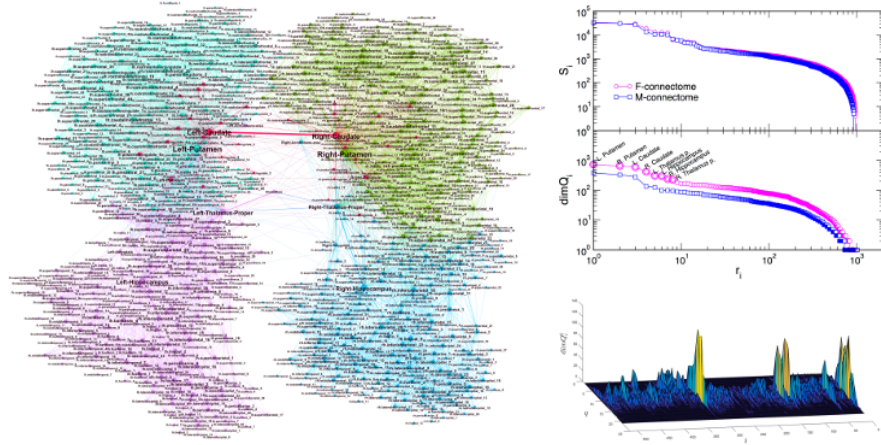


Figure 1: (left) F-connectome, 1000K fibres, with labels as brain areas. (right, top) Ranking of the vertices according to the strength  $S_i$ , top, and topological dimension  $dimQ_i$ , lower panel, where eight leading vertices are marked (they also visible as hubs in the network on the left). (right, bottom) The 3D plot of the topological dimension against the topology level  $q$  and the node's index  $i$  for nodes in the F-core graph.

Next, we consider a reduced network consisting of these hubs and the nodes directly attached to any one of the hubs, as well as the original edges between them in the F- and M-connectomes. The resulting *core networks* termed Fc- and Mc-networks, respectively, are shown in figure 2. Note that, by definition, the topological dimension of the hubs is invariant to this network reduction.

### 3.2 Core networks associated with global hubs in the female and male connectomes

The extracted core Fc- and Mc-networks represent the part of the corresponding connectome in which the global hubs perform their function. Here, we explore in detail the structure of the core networks in the female and male connectomes. Furthermore, we analyse how the structure depends on the weights of the edges. The histogram of the weights is shown in figure 3a for both Fc- and Mc-networks. As figure 2 demonstrates, these core networks exhibit a similar community structure. Precisely, each community in the Fc- and similarly in Mc-connectome is a part of the global connectome community, cf. figure 1. This fact suggests that, in both connectomes, the core network reaches to all parts of the brain. Meanwhile, it contains a smaller number of nodes (517 nodes

in the Fc- and 418 in the Mc-network, respectively), and a considerably smaller number of connections compared to the whole connectome. Thus, the node’s assortativity changes as compared to the whole network. As the inset to figure 3 shows, the hubs mix in line with other vertices in the core graphs, while they make a separate group when the whole connectomes are considered [1]. This assortative dependence emphasises the robustness of core networks with respect to the hierarchical transmission of information among brain regions [39].

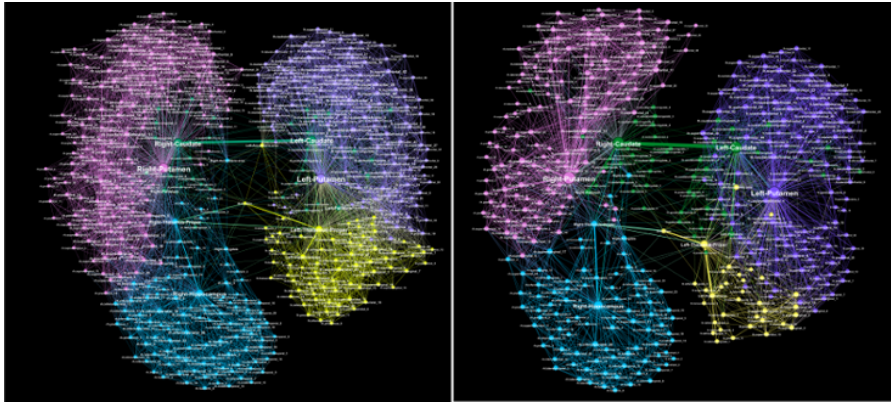


Figure 2: Core networks attached to the eight hubs in the female Fc- (left) and male Mc-connectome (right) from the original full-connectomes data at  $N_F = 10^6$  fibres tracked and the weight threshold  $w_0 = 4$ . The relative size of nodes is proportional to the number of their connections in the core-networks; the node’s labels show the corresponding anatomical brain region, and colours indicate five communities.

### 3.3 Topology of core networks depending on the weights of edges

Using the approaches described in Methods, we determine several algebraic-topology measures to characterise the structure of simplicial complexes as well as the underlying topological graphs in the core Fc- and Mc-networks. These results are summarised in figures 3 and 5. Apart from a different number of nodes and edges that comprise the Fc- and Mc-networks, we note that both of them are heterogeneous concerning the weight of edges, resulting in the broad log-normal distributions in figure 3a. Therefore, we obtain different structures when the edges over a given threshold weight,  $w_0$ , are considered. By gradually increasing the threshold  $w_0 = 10, 40, 100$ , we show how the network properties change. More precisely, by removing the edges below the threshold, the network’s diameter increases, and the distribution of the shortest-path distances change the shape. Eventually, a larger cycle can appear, resulting in the increased value of the hyperbolicity parameter, as shown in figure 3b,c. Meanwhile, the reduced networks preserve the assortative mixing among the nodes, see the inset to figure 3a.



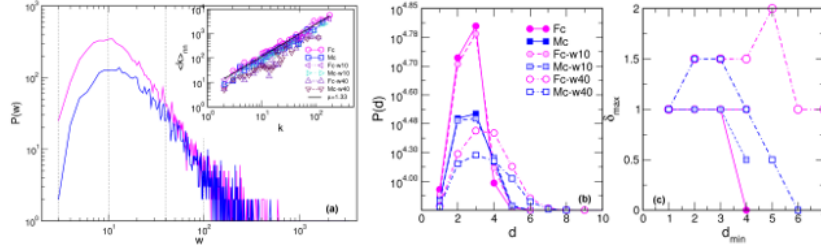


Figure 3: (a) Histogram of the weights of edges in the core Fc - and Mc-networks of the corresponding female and male connectomes, main panel; Inset: the assortativity plots of nodes in the core Fc- and Mc-networks for the weight threshold  $w_0=4, 10, 40$ , and 100, respectively, indicated by dotted vertical lines in the main panel. (b) Distribution of distances  $P(d)$  against the shortest path distance  $d$  and (c) the hyperbolicity parameter  $\delta_{max}$  against the shortest distance  $d_{min}$  for the core Fc- and Mc-networks shown in figure 2, and these networks for two larger threshold weights, indicated in the legend.

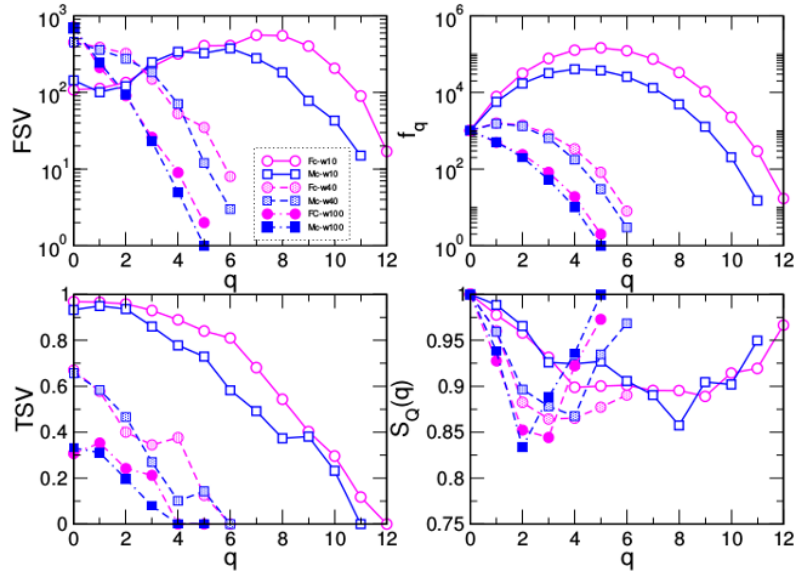


Figure 4: The first (FSV) and third (TSV) structure vectors, the number of simplexes and faces  $f_q$ , and the topological entropy  $S_Q(q)$  against the topology level  $q$  in the core Fc- and Mc-networks with the edges of weights above the threshold  $w_0 = 10, 40, 100$ .

At the same time, the order of simplicial complexes gradually reduces from  $q_{max} = 12$ , in the case of  $w_0 = 10$ , to  $q_{max} = 5$  when edges over the threshold  $w_0 = 100$  are retained. The number of simplexes of the order  $q = 0, 1, 2, \dots, q_{max}$ , given by the FSV, and the ways that they interconnect, the TSV, change the functional dependence of  $q$

while at the same time reducing the difference between the Fc- and Mc-structures, cf. figure 5. The number of simplexes and faces at the  $q$ -level,  $f_q$ , and the topological entropy,  $S_Q(q)$ , follow a similar tendency. Moreover, the topological entropy measure shows a pronounced minimum, indicating the geometrical forms through which the nodes mostly interconnect. For example, in the case of  $w_0 = 100$ , the minimum appears at  $q = 2$  (triangles) in the Mc-, and  $q = 3$  (tetrahedrons) in the Fc-networks, respectively. Figure 5 illustrates the remaining structures of the Fc- and Mc-networks when the weight threshold  $w_0 = 40$  is applied.



Figure 5: Core networks with the weights of edges above  $w_0 = 40$  for the female (left) and male (right) connectomes. Labels of nodes indicate the affected brain regions.

An edge-to-edge comparison between the core Fc- and Mc-networks with the threshold weight  $w_0 = 40$ , shown in figure 5, revealed 948 edges that appear in both of them. Besides, the core Mc-network has 204 unique edges that are not present in the Fc-network with this threshold value, while the Fc-network has 419 such edges that are not seen in the corresponding Mc-network. Moreover, the weight difference among the common edges varies, as shown in figure 6. For example, the pairs of nodes that make up 16 edges with a large difference  $|w_M - w_F| > 300$  are listed below:

ID	src_node	ID	dst_node	w_M	w_F
51	rh.parsopercularis_2	504	Right-Putamen	601	980
151	rh.precentral_9	504	Right-Putamen	740	375
159	rh.precentral_7	504	Right-Putamen	2453	1544
502	Right-Thalamus-Pr.	1008	Left-Thalamus-Pr.	809	1721
503	Right-Caudate	504	Right-Putamen	3340	2843
503	Right-Caudate	505	Right-Pallidum	3072	2280
503	Right-Caudate	507	Right-Hippocampus	937	591
503	Right-Caudate	1009	Left-Caudate	7122	8211
651	lh.precentral_21	1010	Left-Putamen	1220	765
654	lh.precentral_16	1008	Left-Thalamus-Pr.	137	584
654	lh.precentral_16	1010	Left-Putamen	1460	631
657	lh.precentral_4	1010	Left-Putamen	1796	993
661	lh.precentral_6	1010	Left-Putamen	618	1084
1008	Left-Thalamus-Pr.	1013	Left-Hippocampus	2481	2917
1009	Left-Caudate	1010	Left-Putamen	3174	2362

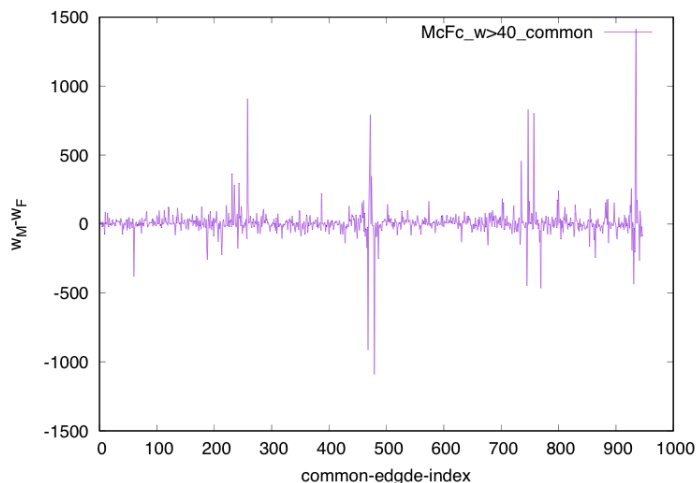


Figure 6: The weight difference  $w_M - w_F$  of the common edges, indexed from 1 to 948, in the Fc- and Mc-core networks in Fig. 5 with the edges weight over 40.

## 4 Discussion and Conclusions

We have analysed the structure of simplicial complexes surrounding eight topological hubs in the human connectomes. The hubs here determined as the top-ranking nodes with the highest topological dimension (the number of simplexes attached). They represent the central brain regions that coincide with the hubs determined by several other graph-theoretic measures. By parallel analysis of the female and male consensus connectomes, we have extracted the corresponding core segments, here termed the Fc- and Mc-networks, in which the brain hubs perform their function. Further, we have demonstrated that these core networks are heterogeneous concerning the weights of edges and they possess different weight-dependent organisations. Consequently, their structure simplifies with the increased weight threshold, eventually reducing at significant thresholds to the 6-clique structure. Interestingly, these six nodes

`Right_Thalamus_Proper, Right_Caudate, Right_Putamen,`  
`Right_Pallidum, Right_Hippocampus, Right_Amygdala`

make up a remaining 6-clique structure in both female and male core networks. With two additional nodes, we have found another 6-clique in the female core network, i.e.,

`rh.precentral_15, rh.precentral_7, Right_Thalamus_Proper,`  
`Right_Caudate, Right_Putamen, Right_Pallidum`

In both core networks, the identity of the affected brain regions, as well as the variation of the weights along the commonly present edges, illustrates further differences between the female and male connectomes at the level of hubs.

In the context of higher-order connectivity, these findings can contribute to better understanding the pattern of connections that enable the brain hubs to perform their role in the female and male connectomes. Besides, the revealed detailed structure of simplicial complexes and the identified brain regions that take part in them can facilitate the desired simplex-based dynamics modelling of the brain functions.

## References

- [1] Tadić B, Andjelković M and Melnik R. Functional geometry of human connectomes. 2019 *Sci. Rep.* **9**, 12060
- [2] Bianconi G, Rahmede C and Wu Z. Complex quantum network geometries: Evolution and phase transitions. 2015 *Phys. Rev. E* **92**, 022815
- [3] Ikeda S, Kotani M. Materials inspired by mathematics. 2016 *Science and Technology of Advanced Materials* **17**, 253259
- [4] Šuvakov M, Andjelković M and Tadić B. Hidden geometries in networks arising from cooperative self-assembly. 2018 *Sci. Rep.* **8**, 1987
- [5] Skardal P S and Arenas A. Abrupt desynchronization and extensive multistability in globally coupled oscillator simplexes. 2019 *Phys. Rev. Lett.* **122**, 248301
- [6] Milan A P, Torres J J and Bianconi G. Explosive higher-order kuramoto dynamics on simplicial complexes. 2019 *arXiv:1912.04405*
- [7] Mitrović Dankulov M, Tadić B and Melnik R. Spectral properties of hyperbolic networks with tunable aggregation of simplexes. 2019 *Phys. Rev. E* **100**, 012309
- [8] Cinardi N, Rapisarda A and Bianconi G. Quantum statistics in network geometry with fractional flavor. 2019 *arXiv:1902.10035v1*
- [9] Petri G, Expert P, Turkheimer F, Carhart-Harris R, Nutt D, Hellyer P J and Vaccarino F. Homological scaffolds of brain functional networks. 2014 *J. Royal Soc. Interface* **11**, 101
- [10] Reimann M W, Nolte M, Scolamiero M, Turner K, Perin R, Giuseppe Chindemi G, *et al.* Cliques of neurons bound into cavities provide a missing link between structure and function. 2017 *Frontiers in Computational Neuroscience* **11**, 48
- [11] Avena-Koenigsberger A, Misić B and Sporns O. Communication dynamics in complex brain networks. 2018 *Nature Reviews Neuroscience* **19**, 17–33
- [12] Horstmeyer L and Kuehn C. An adaptive voter model on simplicial complexes. 2019 *arXiv:1909.05812*

- [13] Zhang Z, Descoteaux M, Zhang J, Girard G, Chamberland M, Dunson D *et al.* Mapping population-based structural connectomes. 2018 *NeuroImage* **172**, 130–145
- [14] Rubinov M and Sporns O. Complex network measures of brain connectivity: Uses and interpretations. 2010 *NeuroImage* **52(3)**, 1059–1069
- [15] Shen X, Papademetris X and Constable R T. Graph-theory based parcellation of functional subunits in the brain from resting-state fMRI data. 2010 *NeuroImage* **50(3)**, 1027–1035
- [16] Sockeel S, Schwartz D, Plgrini-Issac M and Benali H. Large-scale functional networks identified from resting-state EEG using spatial 2016 *PLoS ONE* **11(1)**, 1–18
- [17] Liu N, Mok C, Witt E E, Pradhan A H, Chen J E and Reiss A L. Nirs-based hyperscanning reveals inter-brain neural synchronization during cooperative jenga game with face-to-face communication. 2016 *Frontiers in Human Neuroscience* **10**, 82
- [18] Lynn C and Bassett D S. The physics of brain network architecture, function, and control. 2019 *Nature Reviews Phys* **1**, 318–332
- [19] Tozzi A. The multidimensional brain. 2019 *Physcs of Life Reviews* **31**, 86–103
- [20] Sporns O. Structure and function of complex brain networks. 2013 *Dialogues Clin. Neurosci.* **15(3)**, 247–62
- [21] Fallani F, De Vico Richardi J, Chavez M and Achard S. Graph analysis of functional brain networks: practical issues in translational neuroscience. 2014 *Phil. Trans. of The Royal Society B–Biological Sciences* **369(1635)**, SI, VNSP20130521
- [22] Szalkai B, Varga B and Grolmusz V. Graph theoretical analysis reveals: Womens brains are better connected than mens. 2015 *PLOS ONE* **10(7)**, 1–30
- [23] Tadić B, Andjelković M, Boshkoska B M and Levnajić Z. Algebraic topology of multi-brain connectivity networks reveals dissimilarity in functional patterns during spoken communications. 2016 *PLOS ONE* **11(11)**, 1–25
- [24] McNab J A, Edlow B L, Witzel T, Huang S Y, Bhat H, Heberlein K, *et al.* The human connectome project and beyond: Initial applications of 300mT/m gradients. 2013 *NeuroImage* **80**, 234–245
- [25] Bertolero M A, Yeo B T T and DEsposito M. The modular and integrative functional architecture of the human brain. 2015 *Proceedings of the National Academy of Sciences* **112(49)**, E6798–E6807
- [26] Betzel R F, Medaglia J D, Papadopoulos L, Baum G L, Gur R, Gur R, *et al.* The modular organization of human anatomical brain networks: Accounting for the cost of wiring. 2017 *Network Neuroscience* **1(1)**, 42–68

- [27] van den Heuvel M P and Sporns O. Rich-club organization of the human connectome. 2011 *Journal of Neuroscience* **31(44)**, 15775–15786
- [28] Baker S T E, Lubman D I, Yücel M, Allen N B, Whittle S, Fulcher B D, Zalesky A and Fornito A. Developmental changes in brain network hub connectivity in late adolescence. 2015 *Journal of Neuroscience* **35(24)**, 9078–9087
- [29] Oldham S and Fornito A. The development of brain network hubs. 2019 *Developmental Cognitive Neuroscience* **36**, 100607
- [30] Achard S, Delon-Martin C, Vértes P E, Renard F, Schenck M, Schneider F, *et al.* Hubs of brain functional networks are radically reorganized in comatose patients. 2012 *Proceedings of the National Academy of Sciences* **109(50)**, 20608–20613
- [31] Budapest reference connectome 3.0.
- [32] Szalkai B, Csaba Kerepesi, Varga B and Grolmusz V. Parameterizable consensus connectomes from the human connectome project: the Budapest reference connectome server v3.0. 2017 *Cognitive Neurodynamics* **11(1)**, 113–116
- [33] Bandelt H J and Chepoi V. Metric graph theory and geometry: a survey, in Goodman, J.E.; Pach, J.; Pollack, R., eds. *Surveys on discrete and computational geometry: Twenty years later* **453**. Providence, RI: AMS, 2008.
- [34] Jonsson J. *Simplicial Complexes of Graphs*. Lecture Notes in Mathematics, Springer-Verlag, Berlin, 2008.
- [35] Freeman L C. Q-analysis and the structure of friendship networks. 1980 *International Journal of Man-Machine Studies* **12(4)**, 367–378
- [36] Andjelković M, Gupte N and B. Tadić B. Hidden geometry of traffic jamming. 2015 *Phys. Rev. E* **91**, 052817
- [37] Dorogovtsev S. *Lectures on Complex Networks*. Oxford University Press, Inc., New York, NY, USA, 2010.
- [38] Bermudo S, Rodriguez J M, Sigarreta J M and Vilaire J-M. Gromov hyperbolic graphs. 2013 *Discrete Mathematics* **313(15)**, 1575–1585
- [39] Vázquez-Rodríguez B, Liu Z-Q, Hagmann P and Mišić B. Signal propagation via cortical hierarchies. 2020 *bioRxiv* bioRxiv preprint doi: <https://doi.org/10.1101/2020.02.15.950907>.

### Acknowledgments

Work supported by the Slovenian Research Agency (research code funding number P1-0044). MA received financial support from the Ministry of Education, Science and Technological Development of the Republic of Serbia. RM is also grateful for the NSERC and CRC programs for their support.